Conditional generation of arbitrary single-mode quantum states of light by repeated photon subtractions

Jaromír Fiurášek,[1,2] Raúl García-Patrón,[1] and Nicolas J. Cerf[1]
[1]*QUIC, Ecole Polytechnique, CP 165, Université Libre de Bruxelles, 1050 Brussels, Belgium*
[2]*Department of Optics, Palacký University, 17. listopadu 50, 77200 Olomouc, Czech Republic*
(Received 15 March 2005; revised manuscript received 7 July 2005; published 23 September 2005)

We propose a scheme for the conditional generation of arbitrary finite superpositions of Fock states in a single mode of a traveling optical field. The setup requires a source of squeezed vacuum states, beam splitters, strong coherent beams, photodetectors with single-photon sensitivity, and a final squeezer. If we want to generate a squeezed superposition of Fock states, which is sufficient in several applications, then the last squeezer is not even needed. The thrust of this method is that it achieves a high fidelity without requiring photodetectors with a high efficiency or a single-photon resolution. The possibility to improve its scaling by using a quantum memory is also discussed.

DOI: 10.1103/PhysRevA.72.033822 PACS number(s): 42.50.Dv, 03.67.−a, 03.65.Wj

I. INTRODUCTION

During recent years, it has been widely recognized that nonclassical states of light represent a valuable resource for numerous applications ranging from ultrahigh precision measurements [1–3] to quantum lithography [4,5] and quantum information processing [6]. It is often desirable to generate nonclassical states of traveling optical modes, as opposed to the cavity QED experiments where the generated state is confined in a cavity and can be probed only indirectly. Many ingenious schemes have been proposed and experimentally demonstrated to generate the single-photon states [7,8] and various multiphoton entangled states such as the GHZ states [9], cluster states [10], and the so-called NOON states [11–15].

Considerable attention has also been devoted to the preparation of arbitrary single-mode states [16–19] and, in particular, the quantum superpositions of coherent states ("Schrodinger cat-like" states) [20,21], which can represent a valuable resource for quantum information processing [22,23]. The experimental generation of arbitrary superpositions of vacuum and single-photon states has been accomplished using parametric down-conversion with the input signal mode prepared in a coherent state [24], employing the quantum scissors scheme [25,26], or conditioning on homodyne measurements on one part of a nonlocal single photon in two spatial modes [27]. It is, however, very difficult to extend these experiments to superpositions involving two or more photons. The known schemes for conditional generation of arbitrary superpositions of Fock states require single-photon sources and/or highly efficient detectors with single-photon resolution, which represents a formidable experimental challenge.

In this paper, we propose a state preparation scheme that does not require single-photon sources and can operate with high fidelity even with low-efficiency detectors that only distinguish the presence or absence of photons. Our scheme is inspired by the proposal of Dakna *et al.* [16], who showed that an arbitrary single-mode state can be engineered starting from vacuum by applying a sequence of displacements and single-photon additions. Our crucial observation is that if the initial state is a squeezed vacuum, then the single-photon addition can be replaced with single-photon subtraction [28,29], which is much more practicable. Indeed, a single-photon subtraction can be achieved by diverting a tiny fraction of the beam with a beam splitter toward a photodetector, so that a click means that a photon has been subtracted from the beam (this process becomes exact for a transmittance tending to 1). In fact, the single-photon subtraction from a squeezed vacuum has already been experimentally demonstrated [30], which provides strong evidence for the practical feasibility of our scheme. We note that the photon subtraction is an extremely useful tool which allows one to generate states suitable for the tests of Bell inequality violation with balanced homodyning [31,32]. It can also be used to improve the performance of dense coding [33], and forms a crucial element of the entanglement distillation schemes for continuous variables [34]. However, the counterpart of using photon subtraction in our preparation scheme lies in the fact that a final antisqueezing operation needs to be performed. The implementation of this operation is technically more involved than the initial squeezed vacuum preparation, although it has already been experimentally demonstrated [35–38]. In addition, a new method based on homodyne detection followed by a feed-forward displacement has been proposed recently [39].

The present paper is organized as follows. In Sec. II, we explain the mechanism of state generation on the simplest nontrivial example of a superposition of vacuum and single-photon states. Our setup then consists of two displacements, one conditional photon subtraction, and two squeezers (squeezing conjugate quadratures). We present the details of the calculation of the Wigner function of the generated state for a realistic setup involving imperfect photon subtraction (obtained with imperfect detectors and beam splitters with a nonunity transmittance). In order to evaluate the performance of the scheme, we investigate the achieved fidelity and the preparation probability for various target states. We also discuss the feasibility of the final squeezing operation. In Sec. III, we extend the scheme to the generation of an

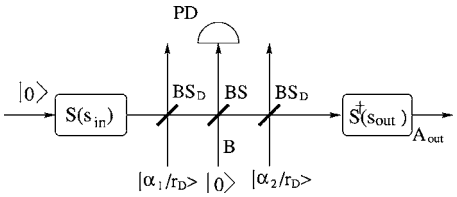

FIG. 1. Proposed experimental setup for generating $|\psi\rangle=c_0|0\rangle+c_1|1\rangle$. An optical parametric amplifier generates a single-mode squeezed vacuum state (of squeezing parameter $s_{\rm in}$), which then propagates through three highly unbalanced beam splitters (BS_D, BS, and BS_D) in order to realize a sequence of two displacements interspersed with one conditional photon subtraction. Finally, an antisqueezing $S^\dagger(s_{\rm out})$ operation is applied, resulting in the output mode $A_{\rm out}$. Successful state preparation is heralded by a click of the photodetector PD.

arbitrary single-mode state and show how to calculate the displacements that need to be applied during the state preparation. As an illustration, we consider the generation of several states which are superpositions of vacuum, single-photon, and two-photon Fock states. In Sec. IV, we propose an iterative state generation scheme that uses a quantum memory in order to reduce very significantly the total number of required operations. Finally, the conclusions are drawn in Sec. V.

II. GENERATION OF A SUPERPOSITION OF $|0\rangle$ AND $|1\rangle$

In this section, we introduce our setup for the generation of an arbitrary superposition of vacuum and single-photon state, which consists of two squeezers and two displacements with a photon subtraction in between, as schematically sketched in Fig. 1. This setup represents a basic building block of our universal scheme: as shown in Sec. III, any superposition of the first $N+1$ Fock states can be generated from a single-mode squeezed vacuum by a displacement followed by a sequence of N photon subtractions and displacements, completed by a final antisqueezing operation.

A. Pure-state description

We first provide a simplified pure-state description of the setup, assuming perfect detectors with single-photon resolution, which will give us an insight into the mechanism of state generation. We will show that, conditionally on observing a click of the photodetector PD, the setup produces a superposition of vacuum and single-photon states,

$$|\psi\rangle_{\rm target}=c_0|0\rangle+c_1|1\rangle. \tag{1}$$

Our state engineering procedure starts with a single-mode squeezed vacuum state, which is generated in an optical parametric amplifier,

$$S(s_{\rm in})|0\rangle=\frac{1}{\sqrt{\cosh(s_{\rm in})}}\sum_{n=0}^{\infty}\frac{\sqrt{(2n)!}}{2^n n!}[\tanh(s_{\rm in})]^n|2n\rangle, \tag{2}$$

where $S(s)=\exp[s(a^{\dagger 2}-a^2)/2]$ denotes the squeezing operator with $a(a^\dagger)$ being the annihilation (creation) operator, and $s_{\rm in}$ denotes the initial squeezing constant. The single-mode squeezed vacuum passes through three highly transmitting beam splitters, which realize a sequence of a displacement followed by a single-photon subtraction and another displacement. The state is displaced by combining it on a highly unbalanced beam splitter BS_D with transmittance $T_D\geq 99\%$ with a strong coherent state $|\alpha/r_D\rangle$, where $r_D=\sqrt{R_D}$ and $R_D=1-T_D$ is the reflectance of BS_D [40]. In the limit $T_D\to 1$, the output beam is displaced by the amount α. This method has been used, e.g., in the continuous-variable quantum teleportation experiments [41]. For the sake of simplicity, we shall assume that $T_D=1$ and the displacement operation is exact. The conditional single-photon subtraction requires a highly unbalanced beam splitter BS with transmittance T, followed by a photodetector PD placed on the auxiliary output port. A successful photon subtraction is heralded by a click of the detector. In the limit $T\to 1$, the most probable event leading to a click of the detector is that exactly a single photon has been reflected from the beam splitter. The probability of removing two or more photons is smaller by a factor of $1-T$ and becomes totally negligible in the limit $T\to 1$. The conditional single-photon subtraction can be described by the nonunitary operator

$$X=t^n r a, \tag{3}$$

where $n=a^\dagger a$ is the photon-number operator, while $t=\sqrt{T}$ and $r=\sqrt{1-T}$ denote the amplitude transmittance and reflectance of BS, respectively.

The input-output transformation corresponding to the sequence of operations in Fig. 1 reads

$$|\psi\rangle_{\rm out}=S^\dagger(s_{\rm out})D(\alpha_2)XD(\alpha_1)S(s_{\rm in})|0\rangle, \tag{4}$$

where $D(\alpha)=\exp(\alpha a^\dagger-\alpha^* a)$ is the displacement operator. We will show later on how the displacements α_1 and α_2 depend on the target state (1), as well as how the output squeezing value $s_{\rm out}$ depends on the initial squeezing $s_{\rm in}$ for a given transmittance $T<1$. But, to make it simple, let us assume first that $T=1$, $\alpha_1=-\alpha_2=\alpha$, and $s_{\rm out}=s_{\rm in}=s$. Then, using $D(\alpha)^\dagger aD(\alpha)=a+\alpha$, the conditionally generated state can be written as

$$|\psi\rangle_{\rm out}=S^\dagger(s)(a+\alpha)S(s)|0\rangle. \tag{5}$$

Taking into account that a and $a^\dagger$ transform under the squeezing operation according to

$$S^\dagger(s)aS(s)=a\cosh(s)+a^\dagger\sinh(s),$$

$$S^\dagger(s)a^\dagger S(s)=a^\dagger\cosh(s)+a\sinh(s), \tag{6}$$

we obtain

$$|\psi\rangle_{\rm out}=[a\cosh(s)+a^\dagger\sinh(s)+\alpha]|0\rangle=\sinh(s)|1\rangle+\alpha|0\rangle. \tag{7}$$

We can see that by setting $\alpha=(c_0/c_1)\sinh(s)$, we obtain the target state (1). This simple analysis illustrates the principle of the scheme shown in Fig. 1. However, the limit $T=1$ is unphysical, because the probability of successful state generation vanishes when $T\to 1$. Let us now take into account $T<1$.

In order to simplify the expression (4), we first rewrite all displacement operators in a normally ordered form, $D(\alpha)=e^{-|\alpha|^2/2}e^{\alpha a^\dagger}e^{-\alpha^* a}$, and we obtain

$$|\psi\rangle_{\rm out} \propto S^\dagger(s_{\rm out})e^{\alpha_2 a^\dagger}e^{-\alpha_2^* a}t^n a e^{\alpha_1 a^\dagger}e^{-\alpha_1^* a}S(s_{\rm in})|0\rangle. \quad (8)$$

Next, we propagate the operator t^n to the right by using the relations

$$t^n e^{\alpha^* a}=e^{\alpha^* a/t}t^n, \quad t^n e^{\alpha a^\dagger}=e^{t\alpha a^\dagger}t^n. \quad (9)$$

After these algebraic manipulations, we obtain

$$|\psi\rangle_{\rm out} \propto S^\dagger(s_{\rm out})e^{\alpha_2 a^\dagger}a e^{t\alpha_1 a^\dagger}e^{-[\alpha_2^*+\alpha_1^*/t]a}t^n S(s_{\rm in})|0\rangle. \quad (10)$$

Note that we have also moved to the right the operator $e^{-\alpha_2^* a}$ and used the fact that $e^{\alpha a^\dagger}e^{\beta^* a}=e^{-\alpha\beta^*}e^{\beta^* a}e^{\alpha a^\dagger}$.

The combined action of the operators $t^n S(s_{\rm in})$ on vacuum produces a single-mode squeezed vacuum state just as without applying t^n but with a lower squeezing constant s satisfying

$$\tanh(s)=t^2\tanh(s_{\rm in}), \quad (11)$$

that is,

$$t^n S(s_{\rm in})|0\rangle \propto S(s)|0\rangle. \quad (12)$$

Finally, we move the operator $e^{\alpha_2 a^\dagger}$ to the right, using the formula $e^{\alpha_2 a^\dagger}a=(a-\alpha_2)e^{\alpha_2 a^\dagger}$, which results in

$$|\psi\rangle_{\rm out} \propto S^\dagger(s_{\rm out})(a-\alpha_2)e^{\delta a^\dagger}e^{-\gamma^* a}S(s)|0\rangle, \quad (13)$$

where $\delta=\alpha_2+t\alpha_1$ and $\gamma=\alpha_2+\alpha_1/t$. With the help of Eq. (6), we can write

$$e^{\delta a^\dagger}e^{-\gamma^* a}S(s)|0\rangle \propto S(s)e^{[\delta\cosh(s)-\gamma^*\sinh(s)]a^\dagger}|0\rangle, \quad (14)$$

which is a state with a generally nonzero coherent displacement. This displacement can be set to zero if α_1 and α_2 satisfy

$$(\alpha_2+t\alpha_1)\cosh(s)=(\alpha_2^*+\alpha_1^*/t)\sinh(s). \quad (15)$$

in which case the output state reads

$$|\psi\rangle_{\rm out} \propto S^\dagger(s_{\rm out})(a-\alpha_2)S(s)|0\rangle. \quad (16)$$

Finally, if we choose $s_{\rm out}=s$, we obtain

$$|\psi\rangle_{\rm out} \propto \sinh(s)|1\rangle-\alpha_2|0\rangle. \quad (17)$$

Thus, the desired superposition of the first two Fock states (1) can be obtained by choosing

$$\alpha_2=-\frac{c_0}{c_1}\sinh(s), \quad (18)$$

$$\alpha_1=t\frac{[\tanh^2(s)-t^2]\alpha_2+(t^2-1)\tanh(s)\alpha_2^*}{t^4-\tanh^2(s)}, \quad (19)$$

where the displacement α_1 has been determined from the condition (15). Note that we may assume that the coefficient c_1 of the Fock state $|1\rangle$ is nonzero; otherwise, no photon subtraction is needed to generate the target state.

B. Final antisqueezing operation

In order to obtain a superposition of Fock states at the output, we need to apply the final antisqueezing operation $S^\dagger(s_{\rm out})$, which squeezes a quadrature conjugate to that squeezed by the first squeezer $S(s_{\rm in})$. This operation can be implemented by injecting the signal beam into a nonlinear medium that is strongly pumped by a laser, as demonstrated in [35–38]. A difficulty of this method lies in the fact that a good spatio-temporal overlap between the signal and the pump beams must be achieved. However, a recently proposed alternative method can be used to avoid this problem. Here, an auxiliary mode that is prepared in a squeezed vacuum state is combined with the signal beam at a beam splitter. The auxiliary mode is then measured with a homodyne detector and the appropriate quadrature of the signal beam is displaced proportionally to the measurement outcome [39]. The great advantage of this latter approach is that it only requires the interference between two beams at a beam splitter, which is much easier to achieve than the direct phase-sensitive deamplification of the signal in a nonlinear medium. A very similar scheme has been in fact successfully demonstrated in the recent experiment of continuous variable quantum erasing [42].

Note that if we remove the last squeezing operation $S^\dagger(s_{\rm out})$, we obtain a simpler optical setup which produces a squeezed superposition of Fock states $S(s_{\rm out})[c_0|0\rangle+c_1|1\rangle]$. In many cases, however, this squeezing may not be an obstacle or may even represent an advantage. For example, the generation of Schrödinger cat states $|\alpha\rangle-|-\alpha\rangle$ can, for small $|\alpha|$, be very well approximated by a squeezed single-photon state $S(s)|1\rangle$ [21,29].

C. Realistic model

We shall now present a more realistic description of the proposed scheme, taking into account that the photodetectors exhibit only single-photon sensitivity, but cannot resolve the number of photons in the mode, and have a detection efficiency $\eta<1$. Such detectors have two outcomes, either a click or a no-click. We model this detector as a sequence of a beam splitter with transmittance η followed by an idealized detector which performs a projection onto the vacuum and the rest of the Hilbert space, $\Pi_0=|0\rangle\langle 0|$ (no click), $\Pi_1=\mathbb{1}-|0\rangle\langle 0|$ (a click).

Similarly to Ref. [31], it is convenient to work in the phase-space representation and consider the transformation of Wigner functions. The setup in Fig. 1 involves two modes, the principal mode A and an auxiliary mode B. Initially, the mode A is in a squeezed vacuum state and the covariance matrix is diagonal, $\gamma_A=\mathrm{diag}(e^{-2s_{\rm in}},e^{2s_{\rm in}})$. The Gaussian Wigner function of the initial state of mode A after the first displacement thus reads

$$W_G(r_A;\Gamma_A,d_A)=\frac{\sqrt{\det\Gamma_A}}{\pi}e^{-(r_A-d_A)^T\Gamma_A(r_A-d_A)}, \quad (20)$$

where $r_A=(x_A,p_A)^T$ is the vector of quadratures of mode A and $d_A=z_1\equiv\sqrt{2}(\mathrm{Re}\,\alpha_1,\mathrm{Im}\,\alpha_1)^T$ is the displacement. The matrix Γ_A is the inverse of the covariance matrix γ_A.

In a second step, the modes A and B are mixed on an unbalanced beam splitter BS and then mode B subsequently passes through a (virtual) beam splitter of transmittance η which models the imperfect detection with efficiency η. This transformation is a Gaussian completely positive (CP) map $\mathcal{M}$, and the resulting state of modes A and B is still a Gaussian state with the Wigner function

$$W_{AB}(r_{AB}) = \frac{\sqrt{\det \Gamma_{AB}}}{\pi^2} e^{-(r_{AB}-d_{AB})^T \Gamma_{AB}(r_{AB}-d_{AB})}, \qquad (21)$$

where $r_{AB}=(x_A,p_A,x_B,p_B)^T$. The vector of the first moments $d_{AB}=(d_A,d_B)^T$ and the covariance matrix $\gamma_{AB}=\Gamma_{AB}^{-1}$ can be expressed in terms of the initial parameters of mode A before the mixing on BS (i.e., z_1 and γ_A) as follows:

$$d_{AB} \equiv \begin{pmatrix} d_A \\ d_B \end{pmatrix} = S \begin{pmatrix} z_1 \\ 0 \end{pmatrix},$$

$$\gamma_{AB} = S(\gamma_A \oplus I_B)S^T + G, \qquad (22)$$

where $S=S_\eta S_{\mathrm{BS}}$, $S_\eta=I_A \oplus \sqrt{\eta} I_B$, and $G=0_A \oplus (1-\eta) I_B$ model the inefficient photodetector, and S_{BS} is a symplectic matrix which describes the coupling of the modes A and B on an unbalanced beam splitter,

$$S_{\mathrm{BS}} = \begin{bmatrix} t & 0 & r & 0 \\ 0 & t & 0 & r \\ -r & 0 & t & 0 \\ 0 & -r & 0 & t \end{bmatrix}. \qquad (23)$$

After the photon subtraction, the density matrix $\rho_{A,\mathrm{out}}$ of mode A conditioned on a click of the photodetector PD measuring the auxiliary mode B becomes

$$\rho_{A,\mathrm{out}} = \mathrm{Tr}_B[\rho_{AB}(\mathbb{1}_A \otimes \Pi_{1,B})], \qquad (24)$$

where Tr_B denotes a partial trace over mode B, and ρ_{AB} is the two-mode density matrix of the Gaussian state characterized by the Wigner function (21). Then, after the second displacement of $z_2 \equiv \sqrt{2}(\mathrm{Re}\ \alpha_2, \mathrm{Im}\ \alpha_2)^T$, the Wigner function of mode A can be written as a linear combination of two Gaussian functions (20), namely

$$W(r)P = C_1 W_G(r;\Gamma_1,d_1) + C_2 W_G(r;\Gamma_2,d_2), \qquad (25)$$

where P is the probability of successful generation of the target state. The expression (25) can be derived by rewriting Eq. (24) in the Wigner representation. One uses the fact that the Wigner function of the POVM element $\Pi_{1,B}$ is a difference of two Gaussian functions,

$$W_{\Pi_1}(r) = \frac{1}{2\pi} - \frac{1}{\pi} e^{-x^2-p^2}, \qquad (26)$$

and that the trace of the product of two operators can be evaluated by integrating the product of their Wigner representations over the phase space.

To define the matrices and vectors appearing in Eq. (25), we first divide the matrix $\Gamma_{AB}=\gamma_{AB}^{-1}$ into four submatrices with respect to the $A|B$ splitting,

$$\Gamma_{AB} = \begin{bmatrix} \Upsilon_A & \sigma \\ \sigma^T & \Upsilon_B \end{bmatrix}. \qquad (27)$$

The correlation matrix Γ_1 and the displacement d_1 appearing in the first term on the right-hand side of Eq. (25) are given by

$$\Gamma_1 = \Upsilon_A - \sigma \Upsilon_B^{-1} \sigma^T,$$

$$d_1 = d_A + z_2,$$

$$C_1 = 1. \qquad (28)$$

Similarly, the formulas for the parameters of the second term read

$$\Gamma_2 = \Upsilon_A - \sigma \tilde{\Upsilon}_B^{-1} \sigma^T,$$

$$d_2 = d_A + \Gamma_2^{-1} \sigma \tilde{\Upsilon}_B^{-1} d_B + z_2,$$

$$C_2 = -2 \sqrt{\frac{\det(\Gamma_{AB})}{\det(\Gamma_2)\det(\tilde{\Upsilon}_B)}} \exp[-d_B^T M d_B], \qquad (29)$$

where $\tilde{\Upsilon}_B=\Upsilon_B+I$ and

$$M = \Upsilon_B \tilde{\Upsilon}_B^{-1} - \tilde{\Upsilon}_B^{-1} \sigma^T \Gamma_2^{-1} \sigma \tilde{\Upsilon}_B^{-1}. \qquad (30)$$

The final squeezing operation $S^\dagger(s_{\mathrm{out}})$, described by the symplectic matrix

$$S_s = \begin{bmatrix} e^{s_{\mathrm{out}}} & 0 \\ 0 & e^{-s_{\mathrm{out}}} \end{bmatrix}, \qquad (31)$$

is applied to mode A after the last displacement. The resulting Wigner function of the output mode A_{out} can be written as

$$W_{\mathrm{out}}(r)P = C_1 W_G(r;\Gamma_1',d_1') + C_2 W_G(r;\Gamma_2',d_2'), \qquad (32)$$

where the inverse covariance matrix $\Gamma_{1,2}'$ and the displacement $d_{1,2}$ appearing in the right-hand side of Eq. (32) are given by

$$\Gamma_{1,2}' = S_s^{-1} \Gamma_{1,2} S_s^{-1},$$

$$d_{1,2}' = S_s d_{1,2}. \qquad (33)$$

Since all the Wigner functions in Eq. (25) or (32) are normalized, the probability of a successful state generation can be calculated simply as the sum $P=C_1+C_2$.

D. Examples

In order to illustrate our method, let us consider the preparation of the following four superpositions of $|0\rangle$ and $|1\rangle$ states:

$$|\psi_1\rangle = |1\rangle, \qquad (34)$$

$$|\psi_2\rangle = \frac{1}{\sqrt{2}}(|0\rangle + |1\rangle), \qquad (35)$$

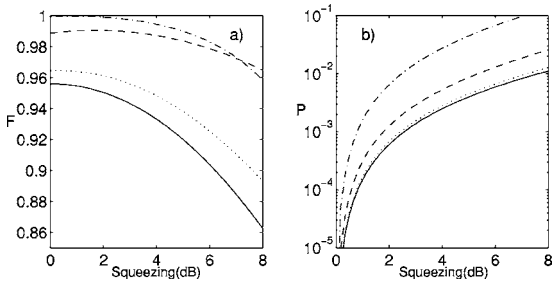

FIG. 2. (a) Fidelity between the generated state and the target state and (b) probability of successful generation as a function of the squeezing s_{in} for the four target states (34) (solid line), (35)(dashed line), (36) (dot-dashed line), and (37) (dotted line), with $T=0.95$ and $\eta=0.25$.

$$|\psi_3\rangle = \frac{1}{\sqrt{10}}(3|0\rangle + |1\rangle), \tag{36}$$

$$|\psi_4\rangle = \frac{1}{\sqrt{10}}(|0\rangle + 3|1\rangle). \tag{37}$$

The fidelity of the generated state for the target states (34)–(37) is plotted in Fig. 2(a) as a function of the initial squeezing. We can see that the conditionally prepared states are close to the desired states and their optimum fidelities are reached for a low initial squeezing (below 2 dB), which is experimentally accessible. Although it is hardly visible in Fig. 2(a), there is typically a nonzero optimal value of the initial squeezing, giving the highest fidelity. As shown in Fig. 2(b), the increase of the initial squeezing improves the probability of successful generation of the target state. A comparison of Fig. 2(a) with Fig. 2(b) reveals a clear trade-off between the achievable fidelity and the preparation probability.

Figure 3(a) shows the dependence of the fidelity on the beam splitter transmittance T, considering the optimal input squeezing for each of the states. [Note that for state (34), we could not find numerically the optimum squeezing, so we arbitrarily chose $s_{\text{in}}=0.50$ dB as an optimal value in other to keep a reasonable generation probability.] We see that as T

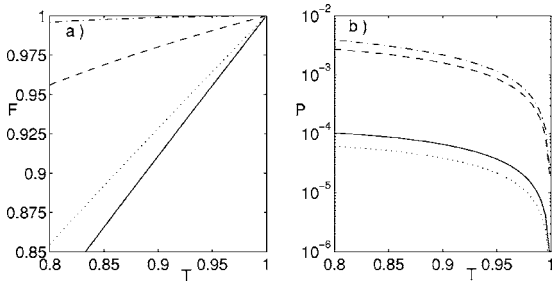

FIG. 3. (a) Fidelity between the generated state and the target state and (b) probability of successful generation as a function of T for the four target states (34)–(37). The curves are plotted considering the optimal squeezing s_{in} for each state, namely 0.50 dB for state (34) (solid line), 1.66 dB for state (35) (dashed line), 0.85 dB for state (36) (dot-dashed line), and 0.36 dB for state (37) (dotted line). The curves are plotted for $\eta=0.25$.

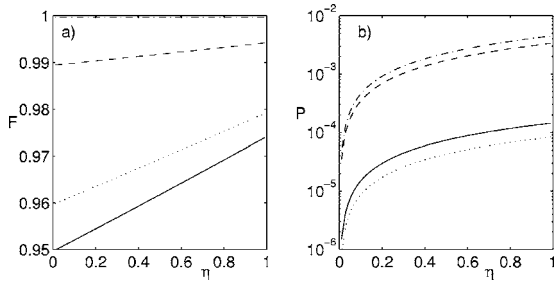

FIG. 4. (a) Fidelity between the generated state and the target state and (b) probability of successful generation as a function of η for the four target states (34)–(37). The curves are plotted considering the optimal squeezing s_{in} for each state, namely 0.50 dB for state (34) (solid line), 1.66 dB for state (35) (dashed line), 0.85 dB for state (36) (dot-dashed line), and 0.36 dB for state (37) (dotted line). The curves are plotted for $T=0.95$.

approaches unity, the fidelity gets arbitrarily close to unity, while the probability of successful state generation decreases as $P \propto (1-T)\eta$, as shown in Fig. 3(b). The value $T=0.95$ used in Fig. 2 seems to be a reasonable compromise between the success rate ($P \approx 10^{-3}$ or $P \approx 10^{-4}$ depending on the target state) and the fidelity, $F \gtrsim 0.95\%$.

We also have studied the dependence of the fidelity on the detection efficiency η. The numerical results are shown in Fig. 4(a), where we can see that the scheme is very robust in the sense that the fidelity almost does not depend on η. Fidelities above 95% could be reached even with η of the order of a few percent if T is high enough. This is in agreement with the findings of Ref. [31]. However, a low η reduces the preparation probability, as shown in Fig. 4(b).

III. ARBITRARY SINGLE-MODE STATE

In the preceding section, we have demonstrated that the combination of two displacements and a photon subtraction allows us to build any superposition of $|0\rangle$ and $|1\rangle$ states. In this section, we shall generalize this procedure to any superposition of the first $N+1$ Fock states,

$$|\psi\rangle_{\text{target}} = \sum_{n=0}^{N} c_n |n\rangle, \tag{38}$$

and show that it can be prepared from a squeezed vacuum state by applying a sequence of $N+1$ displacements interspersed with N photon subtractions, and a final antisqueezing operation as shown in Fig. 5.

A. Pure-state description

As in the preceding section, we first provide a simplified pure-state description of the setup, assuming perfect detectors with single-photon resolution. This will allow us to determine the dependence of the coherent displacements α_j on the target state (38). Generalizing the procedure presented in the preceding section, the input-output transformation corresponding to the sequence of operations in Fig. 5 reads

$$|\psi\rangle_{\text{out}} = S^{\dagger}(s_{\text{out}})D(\alpha_{N+1})XD(\alpha_N)X\cdots D(\alpha_2)XD(\alpha_1)S(s_{\text{in}})|0\rangle. \tag{39}$$

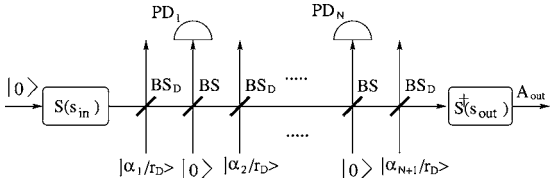

FIG. 5. Proposed experimental setup. An optical parametric amplifier generates a single-mode squeezed vacuum state $S(s_{\rm in})|0\rangle$, which then propagates through $2N+1$ highly unbalanced beam splitters BS_D and BS, which realize a sequence of $N+1$ displacements interspersed with N conditional photon subtractions. A second squeezer is used to apply the final antisqueezing operation $S^\dagger(s_{\rm out})$. Successful state preparation is heralded by clicks of all N photodetectors PD_k.

In order to simplify this expression, we first rewrite all displacement operators in a normally ordered form and then move all the operators t^n to the right using the relations (9). This results in the substitution $\alpha_j \to \alpha_j t^{N+1-j}$ and $\alpha_j^* \to \alpha_j^* t^{j-N-1}$ in the exponents. Next, we propagate all the exponential operators $e^{-t^{j-N-1}\alpha_j^* a}$ to the right,

$$|\psi\rangle_{\rm out} \propto S^\dagger(s_{\rm out}) e^{\alpha_{N+1}a^\dagger} a e^{t\alpha_N a^\dagger} a \cdots a e^{t^N \alpha_1 a^\dagger} e^{-\gamma^* a} t^{Nn} S(s_{\rm in})|0\rangle, \tag{40}$$

where $\gamma=\Sigma_{j=1}^{N+1}\alpha_j t^{j-N-1}$. The combined action of the operators $t^{Nn}S(s_{\rm in})$ on the vacuum produces a single-mode squeezed vacuum state, $t^{Nn}S(s_{\rm in})|0\rangle \propto S(s)|0\rangle$, where $\tanh(s)=t^{2N}\tanh(s_{\rm in})$. After some algebraic manipulations and taking $s_{\rm out}=s$, we get

$$|\psi\rangle_{\rm out} \propto \prod_{j=1}^{N} [a\cosh(s) + a^\dagger \sinh(s) - \beta_j]|0\rangle, \tag{41}$$

where

$$\beta_j = \sum_{k=j+1}^{N+1} \alpha_k t^{N+1-k}. \tag{42}$$

Formula (41) is valid provided that the overall displacement is zero, corresponding to the constraint

$$\cosh(s)\sum_{j=1}^{N+1} \alpha_j t^{N+1-j} = \sinh(s)\sum_{j=1}^{N+1} \alpha_j^* t^{j-N-1}, \tag{43}$$

which generalizes condition (15).

We now prove that an arbitrary superposition of the first $N+1$ Fock states $\Sigma_{n=0}^N c_n|n\rangle$ can be expressed as $\Pi_{j=1}^N(A-\beta_j)|0\rangle \equiv \Sigma_{k=0}^N h_k A^k|0\rangle$, where $A=a\cosh(s)+a^\dagger\sinh(s)$ and h_k are the coefficients of the characteristic polynomial whose roots are β_j. From the condition

$$\sum_{k=0}^{N} h_k A^k|0\rangle = \sum_{n=0}^{N} c_n|n\rangle, \tag{44}$$

we can immediately determine the coefficients h_N and h_{N-1}. This is because only the term A^N gives rise to $a^{\dagger N}$ and, similarly, only the expansion of A^{N-1} contains $a^{\dagger N-1}$. We thus get

$$h_N = \frac{c_N \sinh^{-N}(s)}{\sqrt{N!}}, \quad h_{N-1} = \frac{c_{N-1}\sinh^{1-N}(s)}{\sqrt{(N-1)!}}. \tag{45}$$

Once we know h_N and h_{N-1}, we insert them back in Eq. (44), and, from $\Sigma_{k=0}^{N-2}h_k A^k|0\rangle = \Sigma_{n=0}^N c_n|n\rangle - (h_{N-1}A^{N-1}+h_N A^N)|0\rangle$, we determine h_{N-2} and h_{N-3}. By repeating this procedure, we can find all coefficients h_j. This proves that the condition (44) can always be met for any nonzero squeezing, hence our method is indeed universal and allows us to generate *arbitrary* superpositions. After finding the h_j's, the coefficients β_j's are calculated as the roots of the characteristic polynomial $\Sigma_{k=0}^N h_k\beta^k$, and, finally, the $N+1$ displacements α_j's are determined by solving the system of $N+1$ linear equations (42) and (43).

B. Realistic model

We shall now present a more realistic description of the proposed scheme, which takes into account realistic photodetectors. After kth photon subtraction and $(k+1)$th displacement, the density matrix $\rho_{k,A}$ of mode A conditioned on a click of photodetector measuring the auxiliary mode B is related to $\rho_{k-1,A}$ as follows:

$$\rho_{k,A} = D_{k+1}\mathrm{Tr}_B[\mathcal{M}(\rho_{k-1,A}\otimes|0\rangle_B\langle 0|)(\mathbb{1}_A\otimes\Pi_{1,B})]D_{k+1}^\dagger, \tag{46}$$

where $\rho_{0,A}=D_1 S(s_{\rm in})|0\rangle\langle 0|S^\dagger(s_{\rm in})D_1^\dagger$, $D_{k+1}=D(\alpha_{k+1})$ is a displacement operator, and $\mathcal{M}$ denotes the Gaussian CP map (22) that describes mixing of the modes A and B on BS and accounts for imperfect detection. Since each step (46) gives rise to a linear combination of two Gaussian states from a Gaussian state, the Wigner function of the state $\rho_{k,A}$ can be written as a linear combination of 2^k Gaussian functions,

$$W_k(r)P_k = \sum_{j=1}^{2^k} C_{j,k} W_G(r;\Gamma_{j,k},d_{j,k}), \tag{47}$$

where P_k is the probability of success of the first k photon subtractions. The correlation matrices $\Gamma_{j,k}$ and displacements $d_{j,k}$ after k photon subtractions and $k+1$ displacements can be expressed in terms of $\Gamma_{j,k-1}$ and $d_{j,k-1}$.

Similarly as in Sec. II B, we first define the real displacement vector $z_k \equiv \sqrt{2}(\mathrm{Re}\,\alpha_k, \mathrm{Im}\,\alpha_k)^T$ and the two-mode covariance matrix and vector of mean values after the action of the CP map $\mathcal{M}$,

$$\begin{pmatrix} d_{j,k,A} \\ d_{j,k,B}\end{pmatrix} = S\begin{pmatrix} d_{j,k} \\ 0\end{pmatrix},$$

$$\gamma_{j,k,AB} = S(\Gamma_{j,k}^{-1}\oplus I_B)S^T + G. \tag{48}$$

We also decompose the inverse matrix $\Gamma_{j,k,AB}=\gamma_{j,k,AB}^{-1}$ similarly as in Eq. (27),

$$\Gamma_{j,k,AB} = \begin{bmatrix} \Upsilon_{j,k,A} & \sigma_{j,k} \\ \sigma_{j,k}^T & \Upsilon_{j,k,B}\end{bmatrix}. \tag{49}$$

The jth term in Eq. (47) gives rise to two new terms. The $(2j-1)$th term is parametrized by

$$\Gamma_{2j-1,k} = \Upsilon_{j,k-1,A} - \sigma_{j,k-1}\Upsilon^{-1}_{j,k-1,B}\sigma^{T}_{j,k-1},$$

$$d_{2j-1,k} = d_{j,k-1,A} + z_{k+1},$$

$$C_{2j-1,k} = C_{j,k-1}. \tag{50}$$

Similarly, the formulas for the $2j$th term read

$$\Gamma_{2j,k} = \Upsilon_{j,k-1,A} - \sigma_{j,k-1}\tilde{\Upsilon}^{-1}_{j,k-1,B}\sigma^{T}_{j,k-1},$$

$$d_{2j,k} = d_{j,k-1,A} + \Gamma^{-1}_{2j,k}\sigma_{j,k-1}\tilde{\Upsilon}^{-1}_{j,k-1,B}d_{j,k-1,B} + z_{k+1},$$

$$C_{2j,k} = -2C_{j,k-1}\sqrt{\frac{\det(\Gamma_{j,k-1,AB})}{\det(\Gamma_{2j,k})\det(\tilde{\Upsilon}_{j,k-1,B})}} \times \exp[-d^{T}_{j,k-1,B}Md_{j,k-1,B}], \tag{51}$$

where $\tilde{\Upsilon}_{j,k-1,B} = \Upsilon_{j,k-1,B} + I$ and

$$M = \Upsilon_{j,k-1,B}\tilde{\Upsilon}^{-1}_{j,k-1,B} - \tilde{\Upsilon}^{-1}_{j,k-1,B}\sigma^{T}_{j,k-1}\Gamma^{-1}_{2j,k}\sigma_{j,k-1}\tilde{\Upsilon}^{-1}_{j,k-1,B}.$$

Iterating these formulas N times starting from the initial ($k=0$) Gaussian state (20) and then applying the final antisqueezing operation $S^{\dagger}(s_{\text{out}})$ which acts on the inverse correlation matrices $\Gamma_{j,N}$ and displacements $d_{j,N}$ as in (33), one obtains the Wigner function of the conditionally generated state. The probability of state preparation can be calculated simply as the sum $P=\Sigma_{j=1}^{2^N}C_{j,N}$.

C. Examples

We shall now consider, as an illustration, the generation of superpositions of $|0\rangle$, $|1\rangle$, and $|2\rangle$. These states, namely

$$|\psi\rangle = \frac{1}{\sqrt{1+|c_0|^2+|c_1|^2}}(c_0|0\rangle + c_1|1\rangle + |2\rangle), \tag{52}$$

can be prepared with two photon subtractions. Here, we assume that the coefficient c_2 of the Fock state $|2\rangle$ is nonzero (we arbitrarily take it equal to 1). Otherwise, only one (or zero) photon subtraction would be needed to generate the target state. In the case of two photon subtractions interspersed with three displacements, Eq. (41) reduces to

$$|\psi\rangle_{\text{out}} \propto [\sinh(s)\cosh(s) + \beta_1\beta_2]|0\rangle - (\beta_1+\beta_2)\sinh(s)|1\rangle + \sqrt{2}\sinh^2(s)|2\rangle. \tag{53}$$

This state matches the target state (52) if

$$\beta_{1,2} = \frac{-B \pm \sqrt{B^2-4C}}{2}, \tag{54}$$

where

$$B = \sqrt{2}\sinh(s)c_1,$$

$$C = \sqrt{2}\sinh^2(s)c_0 - \sinh(s)\cosh(s).$$

Equations (42) and (43) allow us to calculate the displacements needed to generate this state. Assuming for simplicity that c_0, c_1, and s are chosen such that β_1 and β_2 are both real, we obtain

$$\alpha_3 = \beta_2,$$

$$\alpha_2 = (\beta_1 - \alpha_3)/t,$$

$$\alpha_1 = \frac{\tanh(s)(\alpha_3 + \alpha_2/t) - (\alpha_3 + t\alpha_2)}{t^2 - \tanh(s)/t^2}. \tag{55}$$

In order to illustrate our method, let us consider the following four superpositions of the Fock states $|0\rangle$, $|1\rangle$, and $|2\rangle$,

$$|\psi_1\rangle = |2\rangle, \tag{56}$$

$$|\psi_2\rangle = \frac{1}{\sqrt{2}}(|1\rangle + |2\rangle), \tag{57}$$

$$|\psi_3\rangle = \frac{1}{\sqrt{2}}(|0\rangle + |2\rangle), \tag{58}$$

$$|\psi_4\rangle = \frac{1}{\sqrt{3}}(|0\rangle + |1\rangle + |2\rangle). \tag{59}$$

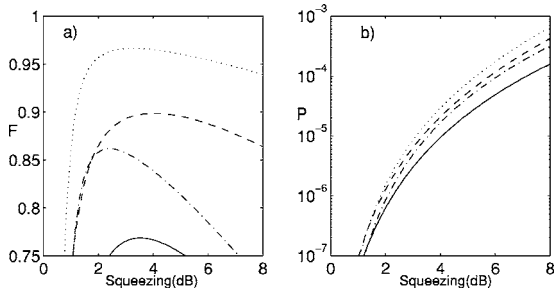

FIG. 6. (a) Fidelity between the generated state and the target state and (b) probability of successful generation as a function of the squeezing s_{in} for the four target states (56) (solid line), (57) (dashed line), (58) (dot-dashed line), and (59) (dotted line), with $T=0.95$ and $\eta=0.25$.

We plot the behavior of the fidelity and probability of generation of the target states (56)–(59) as a function of the initial squeezing s_{in} (Fig. 6), beam-splitter transmittance (Fig. 7), and photodetector efficiency (Fig. 8). As in the preceding section, we observe that the fidelity of the generation for any state gets arbitrarily close to 1 as T approaches unity, as shown in Fig. 7. We also find that the fidelity is very robust against small detector efficiency η, as can be seen in Fig. 8. On the other hand, the preparation probability decreases with a growing T and decreasing η, as predicted by the equation $P \propto (1-T)^2\eta^2$.

All these features are very similar to those found in the preceding section, where we considered only states generated with one photon subtraction. Let us now stress some new features. First, we note here the existence of a clear optimal input squeezing, giving the maximum fidelity for each of the four studied states, see Fig. 6(a). Observing that for a fixed T the optimal squeezing has a higher value [from 2.4 dB for state (58) to 4 dB for state (57)] than those encountered in

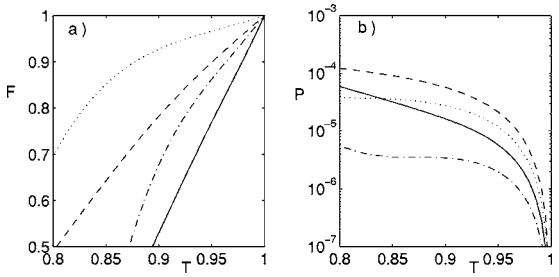

FIG. 7. (a) Fidelity between the generated state and the target state and (b) probability of successful generation as a function of T for the four target states (56)–(59). The curves are plotted considering the optimal squeezing s_{in} for each state, namely 3.54 dB for state (56) (solid line), 4.02 dB for state (57) (dashed line), 2.43 dB for state (58) (dot-dashed line), and 3.24 dB for state (59) (dotted line). The curves are plotted for $\eta=0.25$.

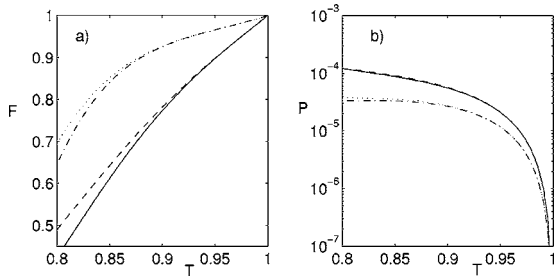

FIG. 9. (a) Fidelity between the generated state and the target state and (b) probability of successful generation as a function of T for the two target states (57) and (59). The curves correspond to the two alternative choices of the displacements α_1 and α_2 when considering the optimal squeezing s_{in} for each state, namely 4.02 dB for state (57) (dotted line, dot-dashed line) and 3.24 dB for state (59) (dashed line, solid line). The curves are plotted for $\eta=0.25$.

the case of one photon subtraction, we can expect an increasing value of the optimal squeezing for an increasing number of Fock states in the target superposition. It can be checked that the value of this optimal input squeezing tends to zero when T tends to 100%, at the expense of a vanishing generation probability.

Another interesting fact is the existence of very different values of the maximum fidelity for different target states for a fixed $T=0.95$ and $\eta=0.25$, as shown in Fig. 6(a). For example, the two-photon state $|2\rangle$ is much more difficult to generate using our method than the other three states (57)–(59). For the state $|2\rangle$, a transmittance of $T\gtrsim 0.99$ is necessary to reach a fidelity of $F\gtrsim 0.95$, resulting in a very low probability of generation. This would make the experimental generation of $|2\rangle$ [or $S(s_{\text{out}})|2\rangle$ if the final squeezing operation is omitted] with a good fidelity very challenging. In contrast, the balanced superposition state (59) can be generated with a high fidelity $F\gtrsim 0.90$ even with a transmittance $T\approx 0.90$.

Finally, a surprising fact arises when $\beta_1\neq\beta_2$. Then, Eq. (55) give two distinct sets of α_i's generating the same target state, the second set being obtained by making the exchange $\beta_1\leftrightarrow\beta_2$. Considering the pure-state description and $T\rightarrow 1$, the two alternative choices of displacements become strictly equivalent. In contrast, when considering the realistic model with $T<1$, these two solutions for the same target state do not have exactly the same behavior. As we can see in Fig. 9(a), one of the two solutions is indeed more robust to decreasing T. However, the two solutions are rather similar as far as the probability of state generation is concerned, as shown in Fig. 9(b).

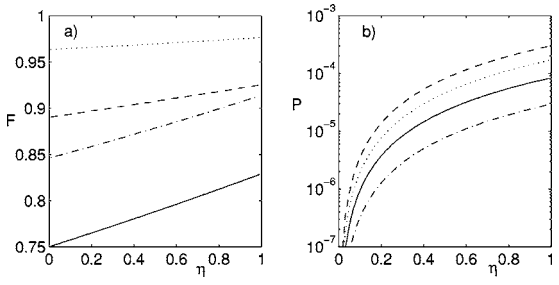

FIG. 8. (a) Fidelity between the generated state and the target state and (b) probability of successful generation as a function of η for the four target states (56)–(59). The curves are plotted considering the optimal squeezing s_{in} for each state, namely 3.54 dB for state (56) (solid line), 4.02 dB for state (57) (dashed line), 2.43 dB for state (58) (dot-dashed line), and 3.24 dB for state (59) (dotted line). The curves are plotted for $T=0.95$.

IV. EFFICIENT STATE PREPARATION USING QUANTUM MEMORY

We have seen in the preceding sections that the probability of successful state preparation decreases exponentially with the maximum number of photons N in the superposition, $P\propto(1-T)^N\eta^N$, which would limit the applicability of the scheme to $N\leqslant 2$ in practice. In order to overcome this problem and enhance the success rate, we have to use some additional resources besides linear optics and squeezers. The main weakness of the present scheme is that all photon subtractions have to succeed simultaneously for the state to be generated, which results in this exponential scaling. As we will see, this can be avoided provided that a quantum memory is employed. Recently, the first experimental demonstrations of quantum memory for light based on the interaction of light beams with atomic ensembles have been reported [43,44]. A quantum memory enables us to deterministically store the state of a light mode for some time, and to retrieve it later on when required.

Our efficient state preparation scheme works in an iterative manner, with two states with up to $N/2$ photons being generated separately and stored in a quantum memory. The total number of trials required to generate both states then scales as $1/P_A+1/P_B$, instead of $1/(P_AP_B)$, which would be the case without a memory. The two states are then merged, and a state with up to N photons is produced. This merging is achieved conditionally by combining the two modes on a balanced beam splitter and projecting one of the output modes onto vacuum, see Fig. 10(a). This requires an efficient detector, being able to discriminate between the presence and absence of a photon. This is a second extra resource for our efficient state preparation scheme. The scheme is iterative in

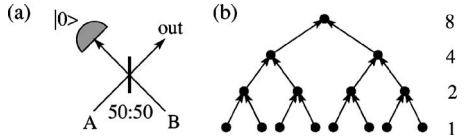

FIG. 10. (a) Setup for merging two states in modes A and B into a single state. The procedure succeeds conditionally on detecting no photons in the left output mode. (b) Starting from superpositions of $|0\rangle$ and $|1\rangle$ and repeating the merging operation iteratively, it is possible to prepare states with up to 2^n photons after n iterations.

the sense that each of the states with up to $N/2$ photons is itself obtained by merging two states with up to $N/4$ photons, etc.

The scheme starts from superpositions of vacuum and single-photon states $c_0|0\rangle+c_1|1\rangle$, which can be prepared conditionally using the scheme discussed in Sec. II. These states are repeatedly merged together and after each successful merging the resulting state is stored in a quantum memory, see Fig. 10(b). After k successful iterations, an arbitrary state containing up to 2^k photons can be prepared. A similar technique was proposed by some of the present authors to efficiently generate two-mode N-photon entangled Schrödinger cat-like states [45], and it is inspired by the quantum repeater concept [46,47] where such a recursive method is exploited to efficiently distribute entanglement through noisy channels over long distances.

In order to check that the iterative scheme is universal, note that any state $|\psi^{(2N)}\rangle=\Sigma_{n=0}^{2N}c_n|n\rangle$ can be written as $|\psi^{(2N)}\rangle\propto\Pi_{j=1}^{2N}(a^\dagger-\alpha_j)|0\rangle$. Now choose $|\psi_A^{(N)}\rangle\propto\Pi_{j=1}^{N}(\sqrt{2}a_A^\dagger-\alpha_j)|0\rangle$ and $|\psi_B^{(N)}\rangle\propto\Pi_{j=N+1}^{2N}(\sqrt{2}a_B^\dagger-\alpha_j)|0\rangle$. If the modes A and B are combined on a balanced beam splitter, then we have in the Heisenberg picture

$$a_{A,\mathrm{in}}=\frac{1}{\sqrt{2}}(a_{A,\mathrm{out}}+a_{B,\mathrm{out}}),$$

$$a_{B,\mathrm{in}}=\frac{1}{\sqrt{2}}(a_{A,\mathrm{out}}-a_{B,\mathrm{out}}). \tag{60}$$

As a consequence, the state of the output mode A conditioned on projecting B onto vacuum is proportional to $|\psi^{(2N)}\rangle$. This decomposition of $|\psi^{(2N)}\rangle$ into $|\psi_A^{(N)}\rangle$ and $|\psi_B^{(N)}\rangle$ can be repeated until we find the $2N$ basic states $c_0^k|0\rangle+c_1^k|1\rangle$, $k=1,\ldots,2N$, from which the state $|\psi^{(2N)}\rangle$ can be iteratively prepared.

As a first example, let us consider the preparation of the state $|\psi^{(2)}\rangle=c_0|0\rangle+c_1|1\rangle+c_2|2\rangle$ by merging the states $a_0|0\rangle+a_1|1\rangle$ and $b_0|0\rangle+b_1|1\rangle$, where the coefficients a_j and b_j can be determined by solving a system of equations

$$\frac{b_1}{b_0}+\frac{a_1}{a_0}=\sqrt{2}\frac{c_1}{c_0},\quad \frac{a_1}{a_0}\frac{b_1}{b_0}=\sqrt{2}\frac{c_2}{c_0} \tag{61}$$

and using the normalization of the states. The probability of successful merging is given by

$$P_M=|a_0|^2|b_0|^2+\frac{1}{2}|a_0b_1+a_1b_0|^2+\frac{1}{2}|a_1|^2|b_1|^2. \tag{62}$$

The probability can be bounded from below, $P_M\geqslant\frac{1}{3}$, and the minimum is achieved when $a_0=b_0=1/\sqrt{3}$ and $a_1=-b_1=\sqrt{2/3}$. It follows that the total number of elementary operations required to generate the state $|\psi^{(2)}\rangle$ is $O_{\mathrm{tot}}\approx 6/P_1$, where P_1 is the probability of preparing the superposition of vacuum and single-photon states. This should be compared with the total number of trials $O_{\mathrm{tot}}\approx 1/P_1^2$ necessary when the scheme described in the preceding section is used instead. As we have seen before, $P_1\approx 10^{-2}$, hence the present procedure reduces the number of necessary operations by more than an order of magnitude even in this simplest case. The price to pay, of course, is the need for a quantum memory and a highly efficient photodetector for the merging operation.

In order to show that the required resources scale only subexponentially with N, let us consider preparation of the single-mode cat-like states $(1/\sqrt{2})(|0\rangle+|N\rangle)$. At the nth iteration step, states $|0\rangle\pm c_{n-1}|2^{n-1}\rangle$ are merged to produce a state $|0\rangle+c_n|2^n\rangle$ (we omitted the normalization prefactors for simplicity). The coefficients are related as follows:

$$c_n=\frac{c_{n-1}^2}{2^{2^{n-1}}2^{n-1}!}\sqrt{2^n!}. \tag{63}$$

Starting from $c_{\log_2 N}=1$, all coefficients c_n, $n<\log_2 N$ can be determined from Eq. (63). The probability of successful merging is given by

$$P_{(n-1)\to n}=\frac{1+|c_n|^2}{(1+|c_{n-1}|^2)^2} \tag{64}$$

and the total number of operations to prepare the state $|0\rangle+c_n|2^n\rangle$ can be estimated as $O_n=2O_{n-1}/P_{n-1\to n}$. For large $K=2^n$, we can use the Stirling approximation $K!\approx\sqrt{2\pi K}K^Ke^{-K}$ and we get $c_n\approx c_{n-1}^2/(\pi 2^{n-1})^{1/4}$. Within this approximation, we can bound the probability (64) as follows:

$$P_{n-1\to n}\approx\frac{1}{\sqrt{\pi 2^{n-1}}}\frac{\sqrt{\pi 2^{n-1}}+|c_{n-1}|^4}{(1+|c_{n-1}|^2)^2}\geqslant\frac{1}{2\sqrt{\pi 2^{n-1}}}. \tag{65}$$

The recurrence formula for the total number of operations becomes $O_n=2\sqrt{\pi 2^{n+1}}O_{n-1}$, which can be solved to yield

$$O_n=\frac{1}{P_1}(2\sqrt{2\pi})^n 2^{n(n+1)/4}, \tag{66}$$

where P_1 is the probability of preparation of $|0\rangle+c_0|1\rangle$. An approximate bound on the total number of operations $O_{\mathrm{cat,tot}}(N)$ required to generate the state $(1/\sqrt{2})(|0\rangle+|N\rangle)$ can be obtained from Eq. (66) by setting $n=\log_2 N$, and we get

$$O_{\mathrm{cat,tot}}(N)\leqslant\frac{1}{P_1}N^{(7/4)+(1/2)\log_2\pi}N^{(1/4)\log_2 N}, \tag{67}$$

which is clearly a subexponential scaling with N. In Fig. 11, we plot the total number of operations as a function of N determined by exact numerical calculations. The log-log plot

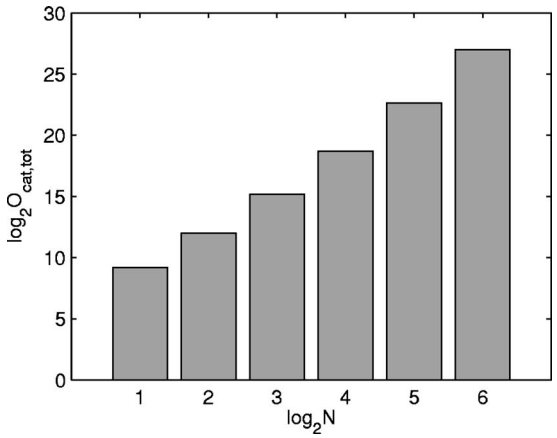

FIG. 11. Total number of operations required to prepare a single-mode Schrödinger cat-like state $(|0\rangle+|N\rangle)/\sqrt{2}$.

reveals that the dependence of $O_{\mathrm{cat,tot}}(N)$ on N is essentially polynomial.

As an example, consider the case $N=8$. Assuming $P_1=10^{-2}$, we get $O_{\mathrm{cat,tot}}(8)=37000$, while if using the scheme discussed in Sec. III, then eight photon subtractions would have to be performed simultaneously and about $(1/P_1)^8=10^{16}$ trials would be required. The scheme employing a quantum memory is thus 11 orders of magnitude more efficient.

V. CONCLUSIONS

In summary, we have shown that an arbitrary single-mode state of light can be engineered starting from a squeezed vacuum state and applying a sequence of displacements and single-photon subtractions, followed by a final squeezing operation. More precisely, the setup based on N single-photon subtractions can be used to generate any superposition of the $N+1$ first Fock states. The experimental implementation of the last squeezing operation may be quite challenging, but actually the scheme remains useful even if it is skipped (in which case the scheme simply produces a squeezed superposition of the $N+1$ first Fock states). Indeed, the generation of squeezed superpositions of Fock states may even represent an advantage in some cases, such as the preparation of Schrödinger cat states.

We have shown that the desired target state can be successfully produced with very high fidelity using a reasonably low squeezing ($\lesssim 3$ dB) if the transmittance T of the beam splitter used for photon subtraction is sufficiently close to unity (e.g., $T\simeq 95\%$). This holds even when inefficient photodetectors with single-photon sensitivity but no single-photon resolution are employed, such as the standard avalanche photodiodes. We have studied the dependence of the achievable fidelity on the detection efficiency η, and have found that the scheme is very robust in the sense that the fidelity almost does not depend on η. Fidelities above 95% could be reached even with η of the order of a few percent if T is high enough. However, low η and high T drastically reduce the preparation probability, so that a compromise has to be made when determining T.

Since our proposal does not require single-photon sources and can operate with low-efficiency photodetectors, we anticipate that its experimental implementation will be much easier than for the previous proposals, in particular the one based on repeated photon additions [16]. The recent demonstration of single-photon subtraction from a single-mode squeezed vacuum [30] provides strong evidence of the practical feasibility of our scheme. In this experiment, a rather low overall detection efficiency ($\eta\approx 1\%$) was reported, due to the spectral and spatial filtering of the beam measured by the photodetector. This filtering is necessary because the optical parametric amplifier emits squeezed vacuum in several modes, while mode A is precisely selected in the experiment by the strong local oscillator pulse in the balanced homodyne detector. Despite this filtering, the single-photon detector PD can sometimes be triggered by photons coming from other modes, so this would probably be the main source of imperfections in our scheme.

Finally, we have demonstrated that the state preparation efficiency can be significantly enhanced by using an iterative scheme starting from superpositions $c_0|0\rangle+c_1|1\rangle$ and merging them together in order to generate higher-dimensional superposition states. This procedure, however, makes the scheme less practicable since it requires a quantum memory and highly efficient detectors discriminating between the presence and absence of photons.

As a conclusion, we may reasonably assert that the generation of arbitrary squeezed superpositions of $|0\rangle$ and $|1\rangle$ should be experimentally achievable using our scheme with the present technology, while some improvement of the filtering and detection efficiency would probably be needed in order to extend the scheme to the preparation of squeezed superpositions of $|0\rangle$, $|1\rangle$, and $|2\rangle$. The final antisqueezing operation required to obtain a finite superposition of Fock states is technically perhaps the most demanding part of the scheme, but is also achievable with the current technology.

ACKNOWLEDGMENTS

We acknowledge financial support from the EU under projects COVAQIAL (FP6-511004) and RESQ (IST-2001-37559), from the Communauté Française de Belgique under Grant No. ARC 00/05-251, and from the IUAP programme of the Belgian government under Grant No. V-18. J.F. also acknowledges support under the Research project Measurement and Information in Optics MSM 6198959213 and from Grant No. 202/05/0498 of the Grant Agency of Czech Republic. R.G-P. acknowledges support from the Belgian foundation FRIA.

[1] B. Yurke, Phys. Rev. Lett. **56**, 1515 (1986); B. Yurke, S. L. McCall, and J. R. Klauder, Phys. Rev. A **33**, 4033 (1986).
[2] M. Hillery and L. Mlodinow, Phys. Rev. A **48**, 1548 (1993).
[3] J. P. Dowling, Phys. Rev. A **57**, 4736 (1998).
[4] A. N. Boto, P. Kok, D. S. Abrams, S. L. Braunstein, C. P. Williams, and J. P. Dowling, Phys. Rev. Lett. **85**, 2733 (2000).
[5] G. Björk, L. L. Sánchez-Soto, and J. Söderholm, Phys. Rev. Lett. **86**, 4516 (2001).
[6] D. Bouwmeester, A. Ekert, and A. Zeilinger, *The Physics of Quantum Information* (Springer, Berlin, 2000).
[7] A. I. Lvovsky, H. Hansen, T. Aichele, O. Benson, J. Mlynek, and S. Schiller, Phys. Rev. Lett. **87**, 050402 (2001).
[8] A. Zavatta, S. Viciani, and M. Bellini, Phys. Rev. A **70**, 053821 (2004).
[9] J. W. Pan, D. Bouwmeester, M. Daniell, H. Weinfurter, and A. Zeilinger, Nature (London) **403**, 515 (2000); J.-W. Pan, M. Daniell, S. Gasparoni, G. Weihs, and A. Zeilinger, Phys. Rev. Lett. **86**, 4435 (2001).
[10] P. Walther, K. J. Resch, T. Rudolph, E. Schenck, H. Weinfurter, V. Vedral, M. Aspelmeyer, and A. Zeilinger, Nature (London) **434**, 169 (2005).
[11] C. C. Gerry, A. Benmoussa, and R. A. Campos, Phys. Rev. A **66**, 013804 (2002).
[12] J. Fiurášek, Phys. Rev. A **65**, 053818 (2002).
[13] H. Lee, P. Kok, N. J. Cerf, and J. P. Dowling, Phys. Rev. A **65**, 030101(R) (2002); P. Kok, H. Lee, and J. P. Dowling, *ibid.* **65**, 052104 (2002).
[14] M. W. Mitchell, J. S. Lundeen, and A. M. Steinberg, Nature (London) **429**, 161 (2004).
[15] H. S. Eisenberg, J. F. Hodelin, G. Khoury, and D. Bouwmeester, Phys. Rev. Lett. **94**, 090502 (2005).
[16] M. Dakna, J. Clausen, L. Knöll, and D.-G. Welsch, Phys. Rev. A **59**, 1658 (1999); **60**, 726 (1999).
[17] J. Clausen, N. Hansen, L. Knoll, J. Mlynek, and D. G. Welsch, Appl. Phys. B: Lasers Opt. **72**, 43 (2001).
[18] C. J. Villas-Boas, Y. Guimaraes, M. H. Y. Moussa, and B. Baseia, Phys. Rev. A **63**, 055801 (2001).
[19] X. B. Zou, K. Pahlke, and W. Mathis, Phys. Lett. A **323**, 329 (2004).
[20] M. Dakna, T. Anhut, T. Opatrný, L. Knöll, and D.-G. Welsch, Phys. Rev. A **55**, 3184 (1997).
[21] A. P. Lund, H. Jeong, T. C. Ralph, and M. S. Kim, Phys. Rev. A **70**, 020101(R) (2004).
[22] H. Jeong and M. S. Kim, Phys. Rev. A **65**, 042305 (2002).
[23] T. C. Ralph, A. Gilchrist, G. J. Milburn, W. J. Munro, and S. Glancy, Phys. Rev. A **68**, 042319 (2003).
[24] K. J. Resch, J. S. Lundeen, and A. M. Steinberg, Phys. Rev. Lett. **88**, 113601 (2002).
[25] D. T. Pegg, L. S. Phillips, and S. M. Barnett, Phys. Rev. Lett. **81**, 1604 (1998); M. Koniorczyk, Z. Kurucz, A. Gábris, and J. Janszky, Phys. Rev. A **62**, 013802 (2000).
[26] S. A. Babichev, J. Ries, and A. I. Lvovsky, Europhys. Lett. **64**, 1 (2003).
[27] S. A. Babichev, B. Brezger, and A. I. Lvovsky, Phys. Rev. Lett. **92**, 047903 (2004).
[28] T. Opatrný, G. Kurizki, and D.-G. Welsch, Phys. Rev. A **61**, 032302 (2000); P. T. Cochrane, T. C. Ralph, and G. J. Milburn, *ibid.* **65**, 062306 (2002); S. Olivares, M. G. A. Paris, and R. Bonifacio, *ibid.* **67**, 032314 (2003).
[29] M. S. Kim, E. Park, P. L. Knight, and H. Jeong, Phys. Rev. A **71**, 043805 (2005).
[30] J. Wenger, R. Tualle-Brouri, and Ph. Grangier, Phys. Rev. Lett. **92**, 153601 (2004).
[31] R. García-Patrón, J. Fiurášek, N. J. Cerf, J. Wenger, R. Tualle-Brouri, and Ph. Grangier, Phys. Rev. Lett. **93**, 130409 (2004); R. García-Patrón, J. Fiurášek, and N. J. Cerf, Phys. Rev. A **71**, 022105 (2005).
[32] H. Nha and H. J. Carmichael, Phys. Rev. Lett. **93**, 020401 (2004).
[33] A. Kitagawa, M. Takeoka, K. Wakui, and M. Sasaki, Phys. Rev. A **72**, 022334 (2005).
[34] D. E. Browne, J. Eisert, S. Scheel, and M. B. Plenio, Phys. Rev. A **67**, 062320 (2003); J. Eisert, D. Browne, S. Scheel, and M. B. Plenio, Ann. Phys. (N.Y.) **311**, 431 (2004).
[35] J. A. Levenson, I. Abram, T. Rivera, P. Fayolle, J. C. Garreau, and P. Grangier, Phys. Rev. Lett. **70**, 267 (1993).
[36] J. P. Poizat and P. Grangier Phys. Rev. Lett. **70**, 271 (1993).
[37] K. Bencheikh, J. A. Levenson, Ph. Grangier, and O. Lopez, Phys. Rev. Lett. **75**, 3422 (1995).
[38] K. Bencheikh, C. Simonneau, and J. A. Levenson, Phys. Rev. Lett. **78**, 34 (1997).
[39] R. Filip, P. Marek, and U. L. Andersen Phys. Rev. A **71**, 042308 (2005).
[40] M. G. A. Paris, Phys. Lett. A **217**, 78 (1996).
[41] A. Furusawa *et al.*, Science **282**, 706 (1998).
[42] U. L. Andersen, O. Glöckl, S. Lorenz, G. Leuchs, and R. Filip, Phys. Rev. Lett. **93**, 100403 (2004).
[43] B. Julsgaard, J. Sherson, J. I. Cirac, J. Fiurášek, and E. S. Polzik, Nature (London) **432**, 482 (2004).
[44] D. N. Matsukevich and A. Kuzmich, Science **306**, 663 (2004).
[45] N. J. Cerf, J. Fiurášek, S. Iblisdir, and S. Massar, in *Proceedings of the 6th International Conference on Quantum Communication, Measurement and Computing*, edited by J. H. Shapiro and O. Hirota (Rinton Press, Princeton, 2003), p. 249.
[46] H. J. Briegel, W. Dür, J. I. Cirac, and P. Zoller, Phys. Rev. Lett. **81**, 5932 (1998).
[47] L. M. Duan, M. D. Lukin, J. I. Cirac, and P. Zoller, Nature (London) **414**, 413 (2001).